Satellite Channel Impairment Mitigation by Diversity Techniques

Peter R. King, Péter Horváth, Fernando Pérez-Fontán,

István Frigyes *Senior Member ,IEEE*, and Stavros Stavrou *Member ,IEEE*

Abstract—**This paper investigates satellite-MIMO, space-time coded for diversity gain. Whereas a dual satellite to single antenna terminal link provides shadowing and some multipath diversity gain, a dual antenna terminal provides additional multipath diversity gain. This gain is demonstrated by simulating high resolution time series channel data for urban and highway environments, for SISO, MISO and MIMO systems, and with uncorrelated and correlated shadowing, and applying it to a bit error rate system simulator using Alamouti space-time coding. Bit error rate curves for each case are provided showing the benefit of 2x2 MIMO over 2x1 MISO. It is shown that 2x1 MISO diversity gain over shadowing (shadow correlation dependent) and multipath diversity gain is of order two (N=2), whereas in the 2x2 MIMO case, diversity gain over shadowing is still of order two but diversity gain over multipath is now of order four (N=4). Methods for investigating shadowing correlation and availability are also given.**

.

Index Terms—**Satellite diversity, MIMO, radio propagation, mobile-satellite communication.**

I. Introduction

FUTURE or current mobile communication systems can benefit from a reliable satellite component to complement the well-established terrestrial link. Key issues associated with a mobile-satellite system are to maintain good coverage availability and QoS by ensuring an adequate signal to noise ratio and maximizing spectral efficiency.

Since in a megacell environment the users are mobile and are expected to operate in urban areas where shadowing effects could be severe, different techniques can be exploited to provide reliable coverage. One way to mitigate the channel impairments is by exploiting diversity between multi satellites and the user's terminal in a MISO system. Furthermore, this paper investigates the MIMO case, channel coded for diversity gain where two antennas at the terminal communicate with two satellites. (A similar setup can also be coded for capacity gain and this is investigated in [1]).

Section II discusses different techniques that can be used to predict signal availability and shadowing correlation. These techniques include ray tracing techniques, the fish-eye picture and street mask techniques. An example of using the street mask technique is presented.

Section III, presents a physical-statistical model for the land mobile-satellite channel, capable of producing joint statistical time series and power-spatial-delay profile data in a multi-antenna mobile, multi-satellite scenario. The model is compared with published measurement data.

Section IV presents some Monte-Carlo simulations to assess the performance gain obtainable by exploiting multiple propagation paths between satellite(s) and the terminal and the bit error rate is compared to the single transmitter-single receiver setup. Simulations are performed on data generated by the physical-statistical model presented in section III.

Section V presents the conclusions of this work.

Manuscript received February 5, 2005. This paper was a result of collaboration within the European Satellite Communications Network of Excellence (SatNEx) framework. The authors wish to thank the SatNEx sponsors for supporting this work.

Peter R. King and Stavros Stavrou are with the Centre for Communication Systems Research, University of Surrey, U.K.

Péter Horváth and István Frigyes are with the Department of Broadband Infocommunication Systems, Budapest University of Technology and Economics. Hungary

Fernando Pérez-Fontán is with the Department of Signal Theory and Communications, University of Vigo, Spain.

II. Multi-satellite diversity

A. Shadowing/blockage path decorrelation

Availability in mobile broadcast and two-way communication satellite systems can be achieved through the use of constellations made up of a number of satellites. These provide different alternative paths from the network to the user terminals thus overcoming blockage and shadowing.

Such constellations must supply sufficiently angle-spaced paths so that decorrelation between blockage effects for the various links is achieved. In [2] measurements of the satellite angular spacing cross-correlation coefficient were reported. A model for built-up areas is presented in [3] that quantifies this coefficient in terms of the masking angle, MKA(º), measured from the centre of the street in the direction perpendicular to its axis. In both references negative correlations were reported for fairly large angle spacings, while sufficient decorrelation was observed for azimuth separations in excess of 40º. Correlation decreases faster if the satellites are seen with different elevations.

B. Satellite availability

For new systems, in the constellation definition stage or while analyzing the locations where terrestrial repeaters or gap-fillers would be required, a number of models have been proposed for built-up areas. The most accurate one is based on ray-tracing techniques performed on building databases, however this technique is costly and time consuming and vegetation is not always available in the database.

Alternative, other simpler techniques have been proposed. One technique utilises a physical-statistical modelling approach like that shown in section III. Another technique is based on the use of fish-eye pictures [4],[5]. These provide a view of the street's "skyline" as seen from the user's point of view, providing an in-detail estimate of the azimuths and elevations for which a connection with a satellite is possible. Analyses of a sufficiently large number of such fish-eye pictures can provide a good estimate of the availability for that particular location and for areas of similar configuration and density.

A geometrical method resembling that of the fish-eye picture approach is based on the so-called street masks [6].

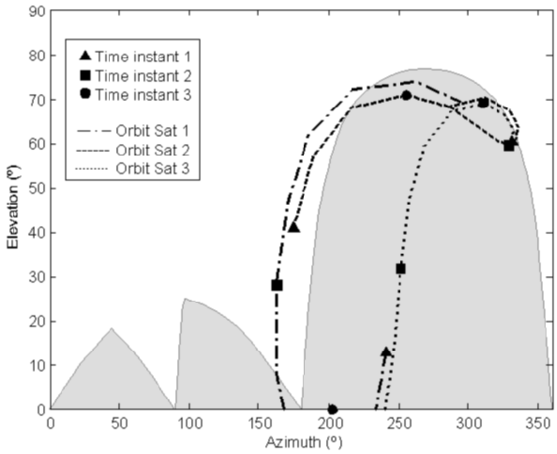

Figure 1: Mask for a t-junction and an MKA=40º. Superposed are the trajectories of the three satellites in the Sirius constellation assuming the terminal is in Boston, USA.

The advantage of masks over fish-eye pictures is that they can be parameterised for any possible density and configuration of the urban environment using the MKA parameter. The disadvantage is that small features showing on the photographs, e.g., lamp posts, as well as trees are not included on the masks.

To illustrate the kind of results that can be obtained using this technique, Figure 1 shows, superposed on the t-junction mask for an urban area with a MKA=40º and a given street orientation, the partial trajectory of the three satellites in the Sirius radio broadcast system constellation. Figure 2 shows the equivalent fish-eye view computed geometrically. The satellite trajectories correspond to a period of 12 hours and the sampling spacing is of one hour. The location chosen was Boston in the USA. To clarify how the mask is applied, three different time-instants marked with a triangle, a square and a circle are shown. The simultaneous satellite positions for a given point in time are marked with the same symbol. Symbols at zero degree elevation correspond to satellite elevations at or below the local horizon. At instants 1 and 2 (triangle and square) two satellites are either below the horizon or inside the shaded zone and one is outside, i.e., it is not blocked. However, at instant 3 (circle) all three satellites are unavailable.

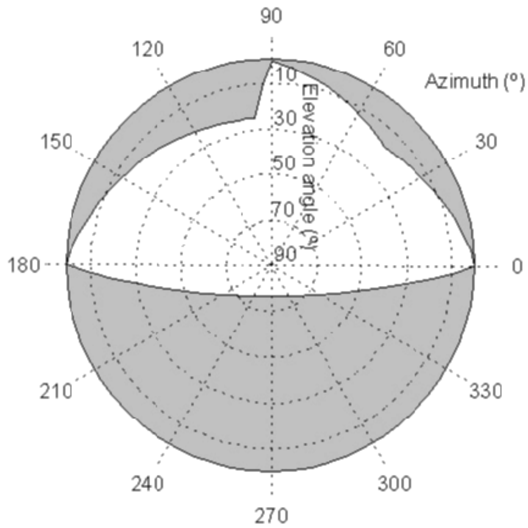

Figure 2: Geometrically calculated equivalent of a fish-eye picture for the same t-junction in Figure 1

Table 1 summarises the availability levels computed for the Sirius system [7], for the four street configurations: canyon, crossing, t-junction and single wall, and for different MKA values.

Table 1. Sirius system availability

MKA	Single Wall	Street Canyon	Street Crossing	T-Junction
10º	1	1	1	1
20º	1	1	1	1
30º	0.9949	0.9880	1	1
40º	0.9522	0.9344	1	1
50º	0.9130	0.8852	0.9961	0.9961
60º	0.8797	0.8295	0.9772	0.9717

III. A MIMO PHYSICAL-STATISTICAL MODEL

A. Model Description and output

This section presents a MIMO land mobile satellite channel model, which is a variation of channel models that trace rays via clusters of scatterers, [8]-[10], but applied to the land mobile-satellite scenario. Once the scatterers are positioned correctly, the model can predict high-resolution time series data and power-spatial-delay profile data between any satellite antenna and any mobile antenna. The model can also predict the correlation between these channels. Positioning the scatterers in each environment is key to the accuracy of the model. To produce enough high-resolution data and a much reduced simulation time, the model has been coded in C++ with the data post-processed in MATLAB. The parameters used in the model are representative of urban and highway environments in Munich, Germany, since published measurement data was available for comparison.

In this model, the clusters of scatterers represent buildings or trees. The cluster centre is randomly positioned above a plane representing the area at half the building or tree height as shown in Figure 3.

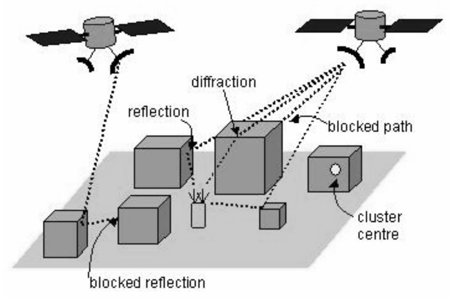

Figure 3: Cluster environment around mobile

Building heights follow a log-normal statistical distribution with a mean and standard deviation derived from best-fit parameters for the city/town. Twenty scatterers were randomly positioned around the cluster centre with each dimension following a Laplacian distribution [8], [11]. Typical densities were estimated to be one building or tree in each $1000m^2$, $1000m^2$ and $10000m^2$ in urban, suburban and highway environments respectively. In the urban environment, clusters were defined as buildings 90% of the time, whereas in the highway environment clusters were defined as trees 90% of the time. In order to simplify the software calculations and increase processing speed, each building or tree width and depth was made equal to its height. This enabled 3D point-line distance vector algebra to be used to establish which scatterers contribute to the overall received electric field. When local clusters, representing buildings, block reflected contributions from distant clusters, the distant clusters are rejected.

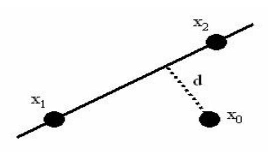

Figure 4: 3D Point-line geometry

For example, in Figure 4, $\mathbf{x_1}$ represents a mobile antenna, and $\mathbf{x_0}$ and $\mathbf{x_2}$ represent cluster centres, whereas **d** is half the building or tree width. When the building obscures the path $\mathbf{x_1}$-$\mathbf{x_2}$, scatterer $\mathbf{x_2}$ is rejected as it is assumed that the building will totally block the signal, and when a tree obscures the path $\mathbf{x_1}$-$\mathbf{x_2}$, scatterer $\mathbf{x_2}$ remains but signal attenuation is applied.

The geometry in Figure 4 is also used for the LOS path. In this case, $\mathbf{x_1}$ represents the mobile antenna and $\mathbf{x_2}$ represents the satellite antenna. When the path $\mathbf{x_1}$-$\mathbf{x_2}$ is blocked by a building or partially blocked by a tree, diffraction loss or tree signal attenuation is applied respectively. For diffraction loss, single knife-edge rooftop diffraction has been adopted for simplicity [16],[17]. For tree loss, the signal reduction is calculated by finding the chord length along path $\mathbf{x_1}$-$\mathbf{x_2}$ and applying 1.3dB/m, an average measured vegetation attenuation [12]-[14].

In 3D space, $\mathbf{x_0} = (x_0,y_0,z_0)$, $\mathbf{x_1} = (x_1,y_1,z_1)$ and $\mathbf{x_2} = (x_2,y_2,z_2)$. After some manipulation, the distance **d** can be found by [14],

$$\mathbf{d} = \frac{\left|(\mathbf{x_2} - \mathbf{x_1}) \times (\mathbf{x_1} - \mathbf{x_0})\right|}{\left|\mathbf{x_2} - \mathbf{x_1}\right|}$$

Rays are traced from the satellite antennas to the mobile antennas via the valid clusters of scatterers. The reflection coefficients are made equal for every scatterer in each cluster and are randomly assigned from a uniform magnitude distribution between 0 and 1 with uniform phase distribution between 0 and 2π. [9].

As the mobile roams, the model switches between three states: a clear LOS path, a blocked LOS path and an attenuated by trees LOS path. The high-resolution time series data between each satellite antenna M and each moving mobile antenna N, $\alpha_{M,N}$ can be defined as follows:

$$\alpha_{M,N} = \begin{cases} P_{M,N} + b.\sum_{i=1}^{n} T_i.\Gamma_i.P_{M,N,i}\,e^{j.k.d_{M,N,i}} & \textit{clear} \\ D_{M,N}.P_{M,N} + b.\sum_{i=1}^{n} T_i.\Gamma_i.P_{M,N,i}\,e^{j.k.d_{M,N,i}} & \textit{blocked} \\ T_{M,N}.P_{M,N} + b.\sum_{i=1}^{n} T_i.\Gamma_i.P_{M,N,i}\,e^{j.k.d_{M,N,i}} & \textit{trees} \end{cases}$$

where $P_{M,N}$ is the LOS path loss between satellite antenna M and moving mobile antenna N, k is the wavenumber, n is the total number of valid scatterers, T_i is the tree attenuation applied to a reflected contribution from scatterer i, Γ_i is the complex reflection coefficient at scatterer i, $P_{M,N,i}$ is the path loss from satellite antenna M to moving mobile antenna N via scatterer i, $d_{M,N,i}$ is the distance between satellite antenna M and moving mobile antenna N via scatterer i, $D_{M,N}$ is the LOS diffraction loss and $T_{M,N}$ is the LOS tree loss. The term b is a clutter factor parameter derived from measurements in each environment.

The model output is high-resolution instantaneous path loss time series data, shown in Figure 5 and power-spatial-delay profile data between each mobile antenna and satellite. From these, the fast-fading statistics can be found as a function of shadowing depth, angle of arrival and arrival distribution, and wideband parameters like RMS delay spread or coherence bandwidth can be estimated in each environment.

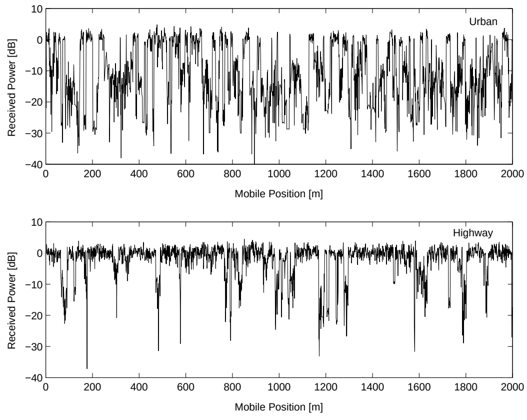

Figure 5: Time series data of model

B. Model Validation

The first order statistics of the high-resolution time series data were also compared with measurements performed by the German Aerospace Centre, DLR [18], and this comparison is shown in Figure 6. The MARECS geostationary satellite at 26°W, transmitting at L-band (1.54 GHz) at an elevation of 24° was used. The urban environment was located in the narrow streets in the old city of Munich, whereas the highway environment was located away from buildings close to Munich. In the urban case, deep shadowing was observed for most of the time. However, for the highway case, only occasional shallow shadowing was observed, caused by trees and rare deep shadowing caused by bridges. The probability levels at each fade-depth and the data trends from the model are in reasonable agreement with the measurement data and therefore the model can be further used to investigate the satellite-MIMO channel.

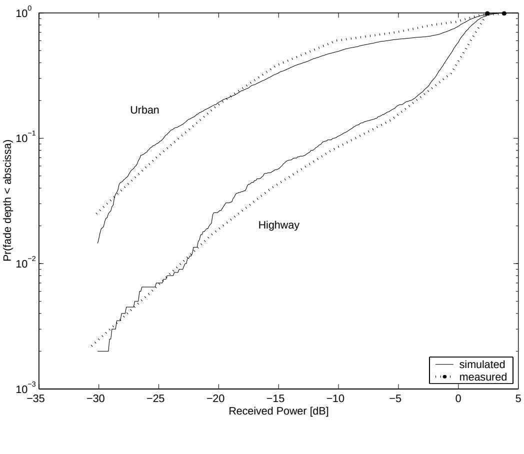

Figure 6: First order statistics of model

The RMS delay spread in the non-shadowed state was calculated from the model to be around 50ns for the urban case; a similar value has been suggested in [19].

IV. Performance improvement through diversity

A. Alamouti's scheme

Monte-Carlo simulations were performed to assess the performance gain obtainable by exploiting multiple propagation paths between the satellite(s) and the user's terminal and the bit error rate is compared to the single transmitter-single receiver setup.

Alamouti's [20] orthogonal space-time block code was used as a means to provide transmit and combined transmit/receive diversity, respectively. This scheme operates on 2-symbol blocks and a simple linear processing detector can be used in the receiver.

Although Alamouti's scheme is originally meant for providing transmit diversity using co-located transmitters, as the streams transmitted from the transmit antennas are orthogonal only if they are perfectly aligned in time. If the transmissions arrive at the receiver at different times, the orthogonality of this coding scheme gets lost. This is especially true if the delay difference is less than the duration of a transmission block (2 symbols), i.e. a block interferes with itself. Moreover, the optimum sampling instant will likely differ for the different transmitters causing additional intersymbol interference. However, it was demonstrated (see e. g. [21]) that using more complex receiver structures and allowing for additional synchronization, it can also be used as a "distributed" transmit diversity scheme. If the receiver uses appropriate equalization (for instance, a generalized MLSE scheme operating on symbol-spaced samples like in [21]) and that equalizer can cope with the effective channel memory, the performance approaches or even reaches that of the perfectly synchronized transmission. In this case other factors limit the maximum allowable delay difference, for example, samples at the matched filter output must be preserved for later processing with proper resolution. This can be prohibitive as the delay difference increases. Limiting the maximum delay difference by using coarse timing advance adjustment between the transmitting satellites can make the transmit diversity feasible.

B. BER curves

Figure 7 and Figure 8 provide BER curves for the synchronous case, which can be considered as a lower bound on the performance. Simulations assume coherent QPSK modulation, flat channel response and quasistatic fading. Results are produced from channel data generated from the physical statistical model of section III, for the urban and highway case. In each of the dual satellite systems, curves are given for both correlated and uncorrelated shadowing cases: shadowing correlation can be found using the techniques shown in section II.

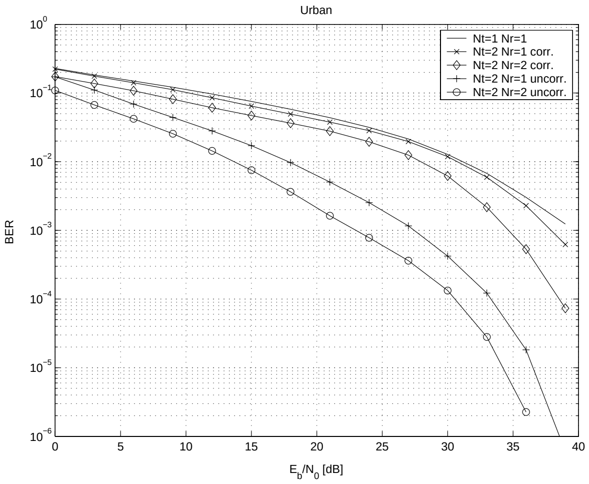

Figure 7: BER for urban case

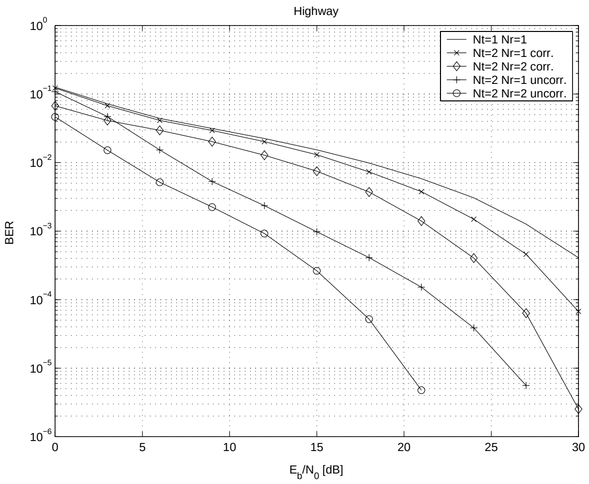

Figure 8: BER for highway case

V. CONCLUSION

This paper has investigated using MIMO technology in the land mobile-satellite environment. MIMO can be space-time channel coded for spatial multiplexing capacity gain or diversity gain or both. Here the benefit of satellite-MIMO coded for diversity gain only is investigated. The benefits are presented in terms of BER curves for urban and highway environments for the cases where the mobile-dual satellite shadowed paths are uncorrelated or correlated. It is shown that additional diversity gain can be exploited from a dual antenna mobile in a 2x2 satellite–MIMO system. Channel coding methods for this ‘distributed’ dual satellite system, with a significant delay offset, have been also described. Estimating shadowing correlation and satellite availability is also investigated by the method of street masks. Satellite-MIMO diversity can lessen the requirement for gap-fillers in some situations and also improve land mobile-satellite quality of service.

REFERENCES

[1] P.R.King, B.G.Evans and S.Stavrou, “Physical-statistical model for the land mobile-satellite channel applied to satellite/HAP MIMO”, European Wireless Conference, April 2005.

[2] A. Jahn, H. Bischl, and G. Heiß. “Channel characterization for spread spectrum satellite communications”. Proc IEEE 4th Symp. Spread Spectrum Tech Appl, ISSSTA, 1996.

[3] M.Vazquez-Castro, F.Perez-Fontan, H.Iglesias-Salgueiro, M.A.Barcia-Fernandez. “A simple 3-segment model for shadowing cross-correlation in multi-satellite systems in street canyons”. Microwave and Optical Technology Letters 2001; 28(3):160–164.

[4] R.Akturan, W.J.Vogel. “Path diversity for LEO satellite PCS in urban environment”. IEEE Transactions on Antennas and Propagation 1997; 45(7):1107–1116.

[5] C.Meenan, M.Parks, R.Tafazolli, B.Evans. “Availability of 1st generation personal communication network service in urban environments”. IEEE Vehicular Technology Conference VTC’98; 1471–1475.

[6] F.Perez-Fontan, M.A.Vazquez-Castro, C.Enjamio, P. Mariño and J.Pita “Approximate urban area call drop-out probability estimation in mobile multi-satellite systems”, Int. J. Satell. Commun. Network. 2003; 21:183–197

[7] F. Davarian. “Sirius Satellite Radio: Radio Entertainment in the Sky”. 2002 IEEE Aerospace Conference

[8] L. M. Correia, “*Wireless Flexible Personalised Communications - Cost 259: European Co-operation in Mobile Radio Research*”, Wiley 2001, pgs 148 – 200

[9] M. Debbah, J. Gil, J. Venes, F. Cardoso, G. Marques and L. M. Correia, “*IST–FLOWS project report D13: Final report on channel models*”, 2003

[10] A. Molisch, “*A Generic Model for MIMO Wireless Propagation Channels in Macro- and Microcells*”, MERL technical report TR2003-042, May 2003.

[11] M. Toeltsch, J. Laurila, K. Kalliola, A. F. Molisch, P. Vainikainen and E. Bonek, “Statistical Characterization of Urban Spatial Radio Channels”, *IEEE Journal on Selected Areas in Communications*, Vol. 20, No. 3, April 2002.

[12] W. Vogel, “Measurement and modeling of land mobile satellite propagation at UHF and L-band”, *IEEE Transactions on Antennas and Propagation*, Vol. 36, No. 5, May 1988.

[13] W. Vogel and J. Goldhirsh, “Mobile satellite system propagation measurements at L-band using MARECS-B2”, *IEEE Transactions on Antennas and Propagation*, Vol. 38, No. 2, Feb. 1990.

[14] I. H. Cavdar, H. Dincer and K. Erdogdu, “Propagation measurements at L-band for land mobile satellite link design”, *Proc. 7th Mediterranean Electrotechnical Conference*, Apr. 1994.

[15] E. W. Weisstein. "Point-Line Distance--3-Dimensional.", MathWorld--A Wolfram Web Resource.

[16] W.C.Y. Lee, *Mobile Comms. Engineering*, McGraw Hill, 1985.

[17] T. S. Rappaport, *Wireless Communications*, Prentice Hall, 1996.

[18] E. Lutz, D. Cygan, M. Dippold, F. Dolainsky and W. Papke, “The land mobile satellite communication channel – recording, statistics, and channel model”, *IEEE Transactions on Vehicular Technology*, Vol. 40, No. 2, May 1991.

[19] B. Belloul, S. R. Saunders, M. A. N. Parks and B. G. Evans, “Measurement and modelling of wideband propagation at L- and S-bands applicable to the LMS channel”, *IEE Proc. Microwaves, Antennas and Propagation*, Vol. 147, No. 2, Apr.2000.

[20] S. M. Alamouti, “A simple transmit diversity technique for wireless communications”, *IEEE J. Select. Areas Commun.*, vol. 16, pp. 1451-1458, Oct. 1998.

[21] J. Mietzner, P. A. Hoeher, M. Sandell, “Compatible improvement of the GSM/EDGE system by means of space-time coding techniques”, *IEEE Trans. Wireless Commun.*, vol. 2, pp. 690-702, July 2003